ARTICLE   OPEN

Sustained Akt signaling in articular chondrocytes causes osteoarthritis via oxidative stress-induced senescence in mice

Jing Xie[1], Jingting Lin[1], Min Wei[2], Yan Teng[1], Qi He[1], Guan Yang[1] and Xiao Yang [1]

Osteoarthritis (OA) is an age-related disorder that is strongly associated with chondrocyte senescence. The causal link between disruptive PTEN/Akt signaling and chondrocyte senescence and the underlying mechanism are unclear. In this study, we found activated Akt signaling in human OA cartilage as well as in a mouse OA model with surgical destabilization of the medial meniscus. Genetic mouse models mimicking sustained Akt signaling in articular chondrocytes via *PTEN* deficiency driven by either *Col2a1-Cre* or *Col2a1-Cre^ERT2* developed OA, whereas restriction of Akt signaling reversed the OA phenotypes in *PTEN*-deficient mice. Mechanistically, prolonged activation of Akt signaling caused an accumulation of reactive oxygen species and triggered chondrocyte senescence as well as a senescence-associated secretory phenotype, whereas chronic administration of the antioxidant N-acetylcysteine suppressed chondrocyte senescence and mitigated OA progression in *PTEN*-deficient mice. Therefore, inhibition of Akt signaling by PTEN is required for the maintenance of articular cartilage. Disrupted Akt signaling in articular chondrocytes triggers oxidative stress-induced chondrocyte senescence and causes OA.

INTRODUCTION

Osteoarthritis (OA) is an age-related disease characterized by articular cartilage degeneration, which is the leading cause of pain and disability worldwide.[1] The serine/threonine kinase Akt is activated by extracellular signals that activate phosphatidylinositol 3-kinase (PI3K), while the phospholipid phosphatase PTEN negatively regulates the activity of Akt by negating the activity of PI3K.[2] PTEN-modulated PI3K/Akt signaling has been widely studied for its central role in physiology and disease, particularly in cancer, where it has become an attractive pharmacological target.[3] Extensive studies have revealed the function of the PTEN/Akt pathway in chondrocytes during endochondral ossification. Deletion of *Akt1* results in delayed calcification,[4–6] while Akt activation in embryonic chondrocytes promotes chondrocyte proliferation and inhibits hypertrophic differentiation.[7–9] However, the in vivo function of Akt signaling in the maintenance of articular cartilage homeostasis and in OA development is largely undefined. Many studies based on in vitro experiments have reported contradictory results regarding the function of Akt signaling in cartilage homeostasis. PI3K/Akt signaling has been shown to play a chondroprotective role by regulating chondrocyte survival, proliferation and extracellular matrix synthesis.[10–12] In contrast, some studies have reported a detrimental effect of the PI3K/Akt pathway on OA, which might be achieved through transduction of procatabolic stimuli or inhibition of articular chondrocyte autophagy.[13,14] Nevertheless, the causal link between disruptive PTEN/Akt signaling in articular chondrocytes and OA pathogenesis is unclear.

Aging is appreciated as a major risk factor for the prevalence of OA.[15] Although senescent chondrocytes are usually found in OA cartilage tissue, the causative role of senescent cells in OA pathogenesis was not established in vivo until recently.[16]

However, little is known about the mechanisms that modulate the senescence of articular chondrocytes. Excessive reactive oxygen species (ROS) have been demonstrated to be inducers of cellular senescence.[17] In OA chondrocytes, ROS-induced oxidative damage has been implicated as the major cause of cellular senescence, as indicated by reduced capacities for chondrocyte proliferation, survival and extracellular matrix (ECM) synthesis, as well as increased production of matrix-degrading enzymes.[18] Insulin/IGF-1/PI3K/Akt/forkhead-box O (FOXO) signaling is a major pathway that regulates ROS generation and cell senescence.[19,20] FoxO transcriptional factors play a chondroprotective role by supporting oxidative stress resistance.[21–23] However, it remains unknown whether Akt signaling serves as a chondroprotective pathway or executes a prosenescence response during OA pathogenesis in vivo.

In the current study, we employed a series of mouse models to investigate the function and relevant mechanisms of Akt signaling in OA development. We provide in vivo genetic evidence that inhibition of Akt signaling by PTEN is required for the maintenance of articular cartilage, which is achieved through inhibition of oxidative stress-induced chondrocyte senescence. These findings will provide new insights into the physiopathologic mechanisms and the relevant pharmacological targets of human OA.

RESULTS

Akt signaling is activated in human OA and experimental OA mouse models

We first examined the level of phosphorylated AKT (p-AKT) in human OA cartilage. In articular cartilages from traumatic knee

[1]State Key Laboratory of Proteomics, Beijing Proteome Research Center, National Center for Protein Sciences (Beijing), Beijing Institute of Lifeomics, Beijing 102206, China and [2]Department of Orthopaedics, Chinese PLA General Hospital, Beijing 100853, China
Correspondence: Guan Yang (yangguan@bmi.ac.cn) or Xiao Yang (yangx@bmi.ac.cn)
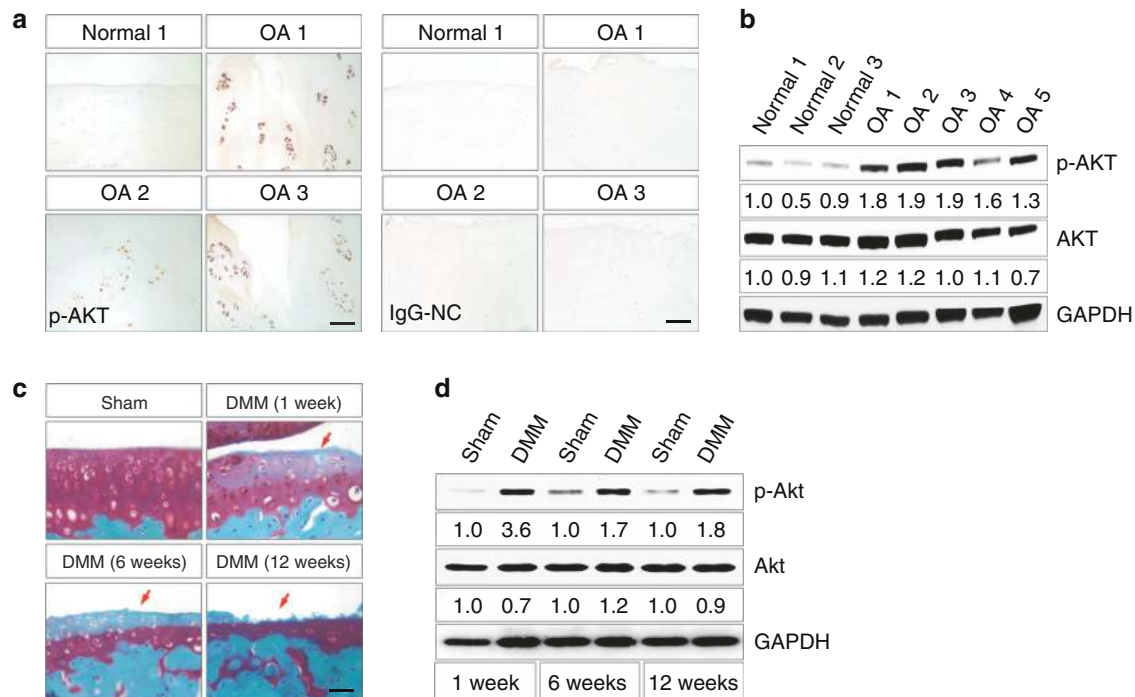These authors contributed equally: Jing Xie, Jingting Lin

Fig. 1 Akt signaling is activated during OA development. **a** Representative images of immunohistochemical staining of p-AKT in human articular cartilage from traumatic knee joints (normal) and knee arthroplasties of OA patients (OA). Nonimmunized rabbit IgG was used as the negative control (IgG-NC). **b** Western blot analysis for p-AKT levels in human normal cartilage and OA cartilage. Quantitative densitometry results are shown below. The GAPDH protein serves as an endogenous normalizer, and the results of each band are then normalized to the value of the "Normal 1" sample. **c** Representative images of safranin O staining of mouse knee joints at 1, 6, and 12 weeks after Sham or DMM surgery performed at 8-week-old ($n = 3$ per group). Arrows denote the articular surface of knee joints that show progressive loss of integrity. **d** Western blot analysis for p-Akt levels in articular cartilage of knee joints at 1, 6, and 12 weeks after Sham or DMM surgery. Quantitative densitometry results are shown below. The GAPDH protein serves as an endogenous normalizer. Scale bars: 100 μm in (**a**); 40 μm in (**c**)

joints, little p-AKT immunohistochemical staining was observed, while in those from knee arthroplasties of OA patients, notable p-AKT staining was present within the clustered articular chondrocytes (Fig. 1a). Western blot analyses confirmed the significantly increased p-AKT level in articular cartilage from OA patients (Fig. 1b), indicating that Akt signaling is activated in human OA chondrocytes.

We then employed a surgical mouse model involving destabilization of the medial meniscus (DMM) to examine the status of Akt signaling during OA development.[24] The histological severity of experimental OA at different stages was demonstrated by safranin O staining (Fig. 1c). The level of p-Akt significantly increased and was sustained with the progression of experimental OA in mice (Fig. 1d). These data demonstrate that Akt signaling is activated during OA pathogenesis.

Sustained Akt signaling in articular chondrocytes causes OA in mice
To determine the contribution of sustained activation of Akt signaling to OA development, we employed a conditional gene knockout mouse (Col2a1-Cre;PTEN$^{fl/fl}$, further referred to as PTEN$^{fl/fl}$) in which the PTEN gene was specifically inactivated in chondrocytes by the Col2a1-Cre transgene.[8] Col2a1-Cre activity in articular chondrocytes was confirmed by the expression of EYFP in Col2a1-Cre;ROSA^{EYFP} reporter mice (ROSA^{EYFP}) (Fig. 2a). Western blot analyses showed decreased levels of PTEN and increased levels of p-Akt in articular cartilage from PTEN$^{fl/fl}$ mice compared to that from control littermates (Col2a1-Cre;PTEN$^{fl/+}$ or Col2a1-Cre, further referred to as Ctrl) at 1, 5 and 10 months of age (Fig. 2b). Reconstructed 3D μCT images of the 8-month-old tibial plateau showed evident roughness and erosion throughout the articular surface of PTEN$^{fl/fl}$ mice, in sharp contrast to that of the Ctrl mice

(Fig. 2c). Histological observation demonstrated evident OA phenotypes in 5-month-old PTEN$^{fl/fl}$ mice. The thickness and organization of articular cartilage deteriorated, in addition to reduced staining for proteoglycan (Fig. 2d). Severe depletion of articular cartilage was observed in 100% of 10-month-old PTEN$^{fl/fl}$ mice (Fig. 2d). OA Research Society International (OARSI) histopathologic scores, including subchondral bone changes, quantified the dramatically increased lesions in PTEN$^{fl/fl}$ articular cartilage as the mice grew older (Fig. 2e). The histopathologic grading of synovial changes, subchondral bone thickening and osteophyte formation also demonstrated the lesions in PTEN$^{fl/fl}$ mice (Supplementary Figs. S1–S3).

We have previously reported dyschondroplasia resulting from PTEN deficiency in the growth plate of PTEN$^{fl/fl}$ mice.[8] Although dyschondroplasia does not occur in articular cartilage, we employed inducible Col2a1-Cre^{ERT2} transgenic mice to exclude the possible influences of growth plate deformities in young PTEN$^{fl/fl}$ mice,[25] and we assessed OA development in Col2a1-Cre^{ERT2}; PTEN$^{fl/fl}$ mutant mice (further referred to as iPTEN$^{fl/fl}$ mice). Five successive doses of tamoxifen injection (Fig. 3a) induced Cre activity in most of the articular chondrocytes of Col2a1-Cre^{ERT}; ROSA^{EYFP} reporter mice (iROSA^{EYFP}) (Fig. 3b). Activation of Akt signaling beyond the key stages of endochondral bone development did not cause visible skeletal defects in 2-month-old iPTEN$^{fl/fl}$ mice (Fig. 3c) but resulted in evident OA phenotypes at 8 months of age (Fig. 3d, e).

We next examined whether OA development in PTEN-deficient mice was primarily caused by Akt activation. We reduced Akt expression in chondrocytes by breeding Col2a1-Cre; PTEN$^{fl/fl}$ mice with Akt1$^{fl/fl}$ mice.[26] Akt1 deletion significantly reduced the total cellular level of Akt protein in articular chondrocytes of Col2a1-Cre; PTEN$^{fl/fl}$;Akt1$^{fl/fl}$ (further referred to as PTEN$^{fl/fl}$;Akt1$^{fl/fl}$) mice (Fig. 4b), indicating that Akt1 was the most highly expressed
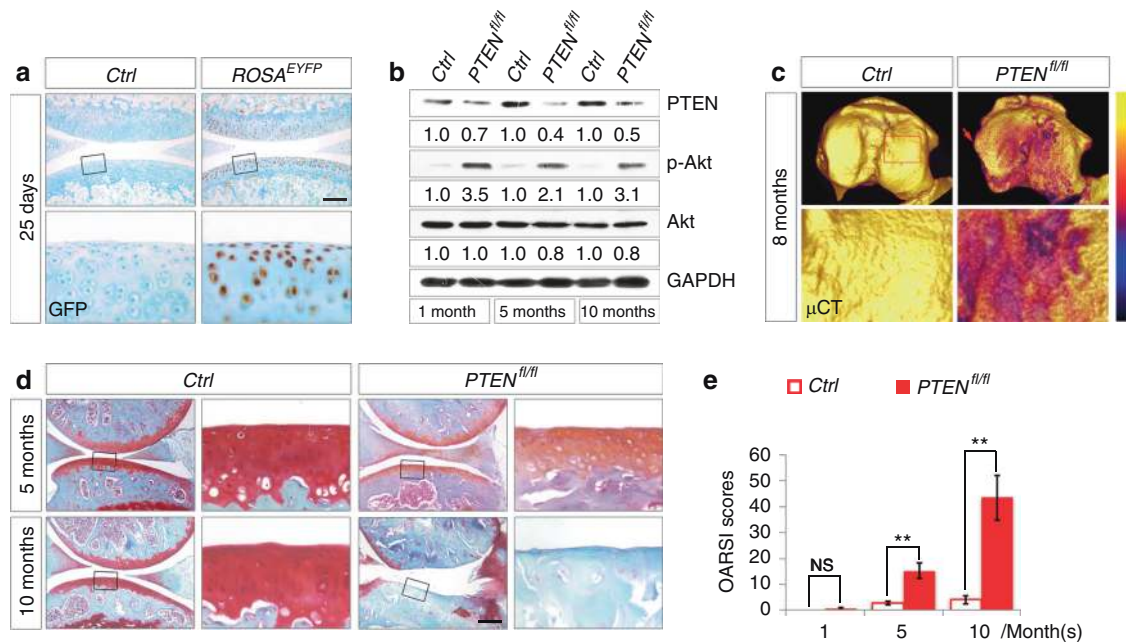
Fig. 2 *PTEN* deficiency in articular chondrocytes causes OA in mice. **a** Representative images of immunohistochemical staining of EYFP in sagittal sections of 25-day-old *Ctrl* and *ROSA*^{EYFP} knee joints ($n = 2$ per group). The framed area in each picture is shown below at a higher magnification. **b** Western blot analyses for the levels of PTEN, Akt, and p-Akt in articular cartilage from *Ctrl* and *PTEN*$^{fl/fl}$ mice at 1, 5, and 10 months. Quantitative densitometry results are shown below. The GAPDH protein serves as an endogenous normalizer. **c** Representative color-coded 3D-reconstructed μCT images of the tibial plateau from *Ctrl* and *PTEN*$^{fl/fl}$ mice at 8 months ($n = 3$ per group). A color scale bar ranging from yellow to black is shown to indicate respective HU values from low to high. The arrow denotes an osteophyte at the medial tibial plateau. The framed area in each picture is shown below at a higher magnification. **d** Representative images of safranin O staining of *Ctrl* and *PTEN*$^{fl/fl}$ knee joints at 5 and 10 months ($n = 8$ per group). The framed area in each picture is shown on the right at a higher magnification. **e** Quantified pathological changes of *Ctrl* and *PTEN*$^{fl/fl}$ knee joints at 1, 5, and 10 months. Each value represents the mean ± SEM ($n = 8$ per group). NS: not significant; **$P < 0.01$. Scale bars: 200 μm in (**a**); 250 μm in (**d**).

isoform in articular chondrocytes. In contrast to the systemic *Akt1*$^{-/-}$ mice,[5] conditional *Col2a1-Cre; Akt1*$^{fl/fl}$ mice appeared normal and did not show visible defects in skeletal development (Supplementary Fig. S4). Interestingly, all *PTEN*$^{fl/fl}$;*Akt1*$^{fl/fl}$ compound-mutant mice displayed a dramatic improvement in articular cartilage integrity, as evidenced by histological examination (Fig. 4a) and OA scores (Fig. 4c). These results demonstrate that *PTEN* deficiency in articular chondrocytes initiates OA development in mice through sustained activation of Akt signaling.

Sustained PI3K/Akt signaling causes oxidative stress-related senescence in articular chondrocytes
The age-related progression of OA phenotypes in *Col2a1-Cre; PTEN*$^{fl/fl}$ mice indicates that chondrocyte senescence might be accelerated by prolonged PI3K/Akt signaling. Oxidative stress induced by ROS is the major cause of chondrocyte senescence.[27] We, therefore, employed OxyIHC to detect protein oxidation in chondrocytes and found that oxidative stress was significantly increased in articular chondrocytes from 4- and 8-month-old *PTEN*$^{fl/fl}$ mice (Fig. 5a, red arrows). The hypertrophy of chondrocytes is also indicative of intracellular ROS.[28,29] In 5-month-old *PTEN*$^{fl/fl}$ mice, the expression of *Col10a1*, a well-established marker for hypertrophic differentiation of chondrocytes, manifested within the articular cartilage and meniscus (Fig. 5b, red arrows). Elevated expression of *Col10a1* mRNA in cartilage from 5- and 10-month-old *PTEN*$^{fl/fl}$ mice was confirmed by real-time PCR (Fig. 5c). OxyBlot is a western blot method that quantifies protein oxidation in tissues based on a principle identical to that of OxyIHC. As shown by OxyBlot, *PTEN* deficiency led to elevated intracellular oxidative stress in articular chondrocytes from 4- and 8-month-old *PTEN*$^{fl/fl}$ mice, which was accompanied by increased levels of p-Akt, p-mTOR, and p-FoxO1/3a (Fig. 5d). Consistently, deletion of *PTEN* triggered senescence of articular chondrocytes, as indicated by SA-β-gal staining within articular chondrocytes (Fig. 5e) as well as elevated levels of the senescence markers p53 and p16 (Fig. 5d). *PTEN*-deficient articular chondrocytes also exhibited a senescence-associated secretory phenotype (SASP), as indicated by elevated expression of *Mmp13* and *Mmp9* (Fig. 5c, f). These results suggest that sustained Akt signaling leads to increased oxidative stress and senescence in articular chondrocytes, which might be responsible for OA pathogenesis.

Antioxidant therapy relieves chondrocyte senescence and mitigates OA phenotypes in *PTEN*$^{fl/fl}$ mice
N-acetylcysteine (NAC) is a classic antioxidant that is well known for its ability to minimize intracellular oxidative stress.[30] Here, we employed long-term intragastric administration of NAC as an antioxidant therapy for the protection of *PTEN*$^{fl/fl}$ chondrocytes from intracellular ROS. Ten milligrams of NAC in 0.9% NaCl solution was administered at 1 month, once every other day until sacrifice. Long-term NAC administration at this dose did not affect viability but slightly reduced the body weight of the mice (data not shown). Histological analysis and OA scoring results showed that NAC treatment effectively reduced articular cartilage degeneration in 10-month-old *PTEN*$^{fl/fl}$ mice compared with that in their *PTEN*$^{fl/fl}$ littermates treated with 0.9% NaCl (Fig. 6a, b). OxyIHC and OxyBlot analyses confirmed the remarkable amelioration of oxidative stress by NAC treatment in chondrocytes from *PTEN*$^{fl/fl}$ mice (Fig. 6c, d). As a result, chondrocyte senescence was dramatically arrested by NAC treatment, as shown by decreased SA-β-gal staining (Fig. 6e) and downregulated p53 levels in *PTEN*-deficient chondrocytes (Fig. 6d). The expression of the OA marker gene *Col10a1* and the SASP marker genes *Mmp13* and *Mmp9* in the articular cartilage of *PTEN*$^{fl/fl}$ mice were also suppressed by NAC treatment (Fig. 6f, g). These results demonstrate that antioxidant therapy diminishes chondrocyte senescence and recovers OA phenotypes in *PTEN*$^{fl/fl}$ mice.
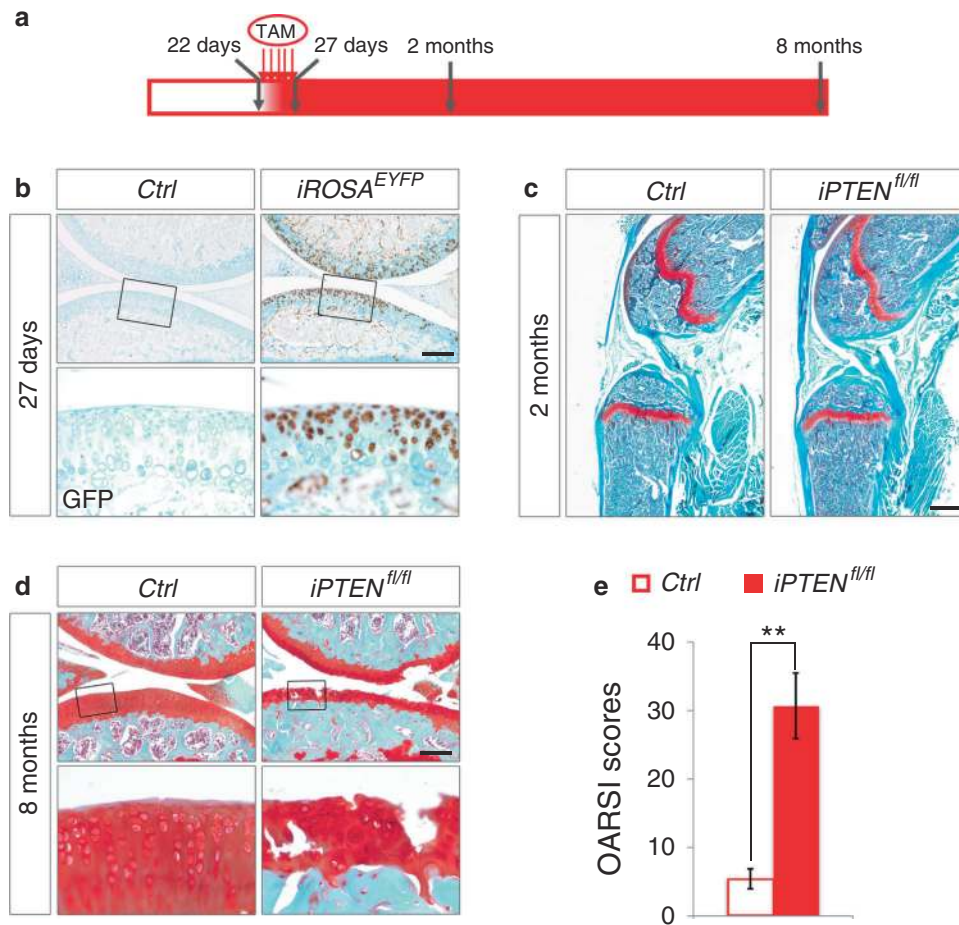
Fig. 3 Induced *PTEN* deficiency in adult articular chondrocytes causes OA phenotypes in mice. **a** Schematic diagram showing the protocol of tamoxifen administration for starting *ROSA*[EYFP] expression or ablating the *PTEN* gene in articular chondrocytes. Five successive doses of tamoxifen were injected every day since 22-day-old. Knee joints were analyzed at 27 days, 2 months and 8 months of age. **b** Representative images of immunohistochemical staining of EYFP in articular cartilage from 27-day-old *Ctrl* and *iROSA*[EYFP] mice ($n = 3$ per group). Tamoxifen was injected since 22-day-old. The framed area in each picture is shown below at a higher magnification. **c** Representative images of safranin O staining of hind limbs from 2-month-old *Ctrl* and *iPTEN*^{fl/fl} mice ($n = 4$ per group). Tamoxifen was injected since 22-day-old. **d** Representative images of safranin O staining of knee joints from 8-month-old *Ctrl* and *iPTEN*^{fl/fl} mice ($n = 12$ per group). Tamoxifen was injected since 22-day-old. The framed area in each picture is shown below at a higher magnification. **e** Quantified pathological changes of each group at 8 months. Each value represents the mean ± SEM ($n = 12$ per group). **$P < 0.01$. Scale bars: 250 μm in (**b**) and (**d**), 800 μm in (**c**)

DISCUSSION

Increasing evidence has shown that cellular senescence plays an important role in aging-related OA development.[16] Deciphering the mechanisms by which chondrocyte senescence is triggered is the key to understanding the pathogenesis of OA. Here, we provide in vivo genetic evidence that inhibition of Akt signaling by PTEN is required for the maintenance of articular cartilage homeostasis. Loss of PTEN in articular chondrocytes leads to sustained Akt signaling and OA via oxidative stress-induced senescence.

Although many studies favor the chondroprotective role of Akt signaling,[10,11,31] we found that in vivo, sustained Akt signaling may deteriorate the integrity of articular cartilage. Akt can transduce both proanabolic and procatabolic signaling in response to diverse stimuli during cartilage repair.[13] Akt signaling may also adopt distinct downstream effectors to perform seemingly opposing functions. For example, mTOR supports protein synthesis and extracellular matrix production during cartilage development and maintenance,[32] while inhibition of mTOR protects cartilage from experimental OA at least in part by supporting autophagy.[33] In this study, we showed that human OA samples and mouse OA models manifested intensive and persistent activation of Akt during OA progression. We further

demonstrated that constitutive or inducible knockout of PTEN in articular chondrocytes led to OA development, providing the first in vivo genetic evidence that prolonged Akt signaling per se is sufficient to initiate OA and suggesting that intrinsic Akt signaling should be appropriately balanced to maintain cartilage integrity.

Our study reveals a prosenescence function of sustained Akt signaling that hampers the integrity of articular cartilage. Targeted elimination of p16[Ink4a]-positive senescent cells in transgenic mice verified their contribution to age-related pathologies and dysfunctions.[34,35] The causal role of senescent chondrocytes in posttraumatic OA pathogenesis has also been addressed using a similar strategy.[16] The prosenescence role of Akt has been suggested in cancer cells and aging *Caenorhabditis elegans*.[36,37] In the current study, we showed that PTEN-deficient articular chondrocytes exhibited high levels of the senescence inducers p16[Ink4a] and p53, senescence-associated β-galactosidase activity and typical features of a SASP, unveiling a mechanism by which the senescence of articular chondrocytes is induced. We further showed that Akt1 knockout significantly rescued the OA phenotypes in PTEN-deficient mice, suggesting that pharmacological inhibition of Akt signaling may be a feasible therapeutic strategy for treating OA.

We show that consistently activated Akt signaling in articular chondrocytes causes OA by oxidative stress-induced senescence.
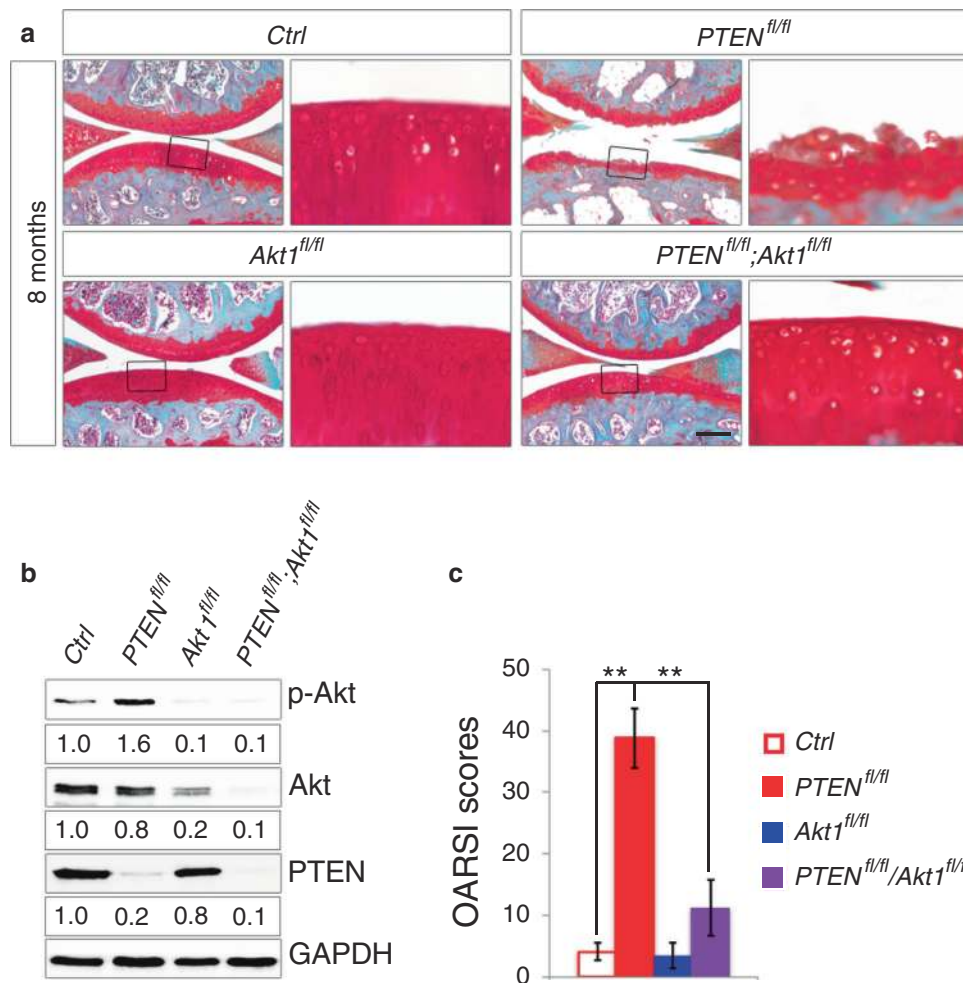
Fig. 4 Genetic inhibition of *Akt1* rescues OA development in *PTEN*-deficient mice. **a** Representative images of safranin O staining of knee joints from each genotype at 8 months ($n = 10$ per group). The framed area in each picture is shown on the right at a higher magnification. **b** Western blot analyses for the levels of p-Akt, Akt and PTEN in articular cartilage from each genotype. Quantitative densitometry results are shown below. The GAPDH protein serves as an endogenous normalizer. **c** Quantified pathological changes in knee joints from each genotype at 8 months of age. Each value represents the mean ± SEM ($n = 10$ per group). **$P < 0.01$. Scale bar: 250 μm

Previous in vitro studies have revealed a correlation between oxidative stress-accelerated chondrocyte senescence and altered Akt signaling in OA chondrocytes.[18,38–40] In this study, *PTEN^{fl/fl}* articular chondrocytes exhibited higher levels of p-mTOR and p-FoxO1/3a, along with elevated oxidative stress and senescence, suggesting a causal role of oxidative stress in OA in *PTEN*-deficient mice. Consistently, systemic application of the antioxidant NAC efficiently relieved articular chondrocytes from oxidative-stress-induced cellular senescence and SASP and largely mitigated the OA phenotypes in *PTEN^{fl/fl}* mice. These findings demonstrate that oxidative stress induced by activated Akt signaling causes chondrocyte senescence and OA, suggesting antioxidants as a potential therapeutic strategy for treating OA. In support of this possibility, very recent preclinical work demonstrates that NAC effectively represses oxidative damage and prevents posttraumatic OA.[41]

MATERIALS AND METHODS

Human articular cartilage specimens
Discarded human articular cartilage from orthopedic surgery patients was sourced from Chinese PLA General Hospital, which included 3 traumatic knee joint specimens from individuals with no history of arthritic diseases and 6 knee arthroplasty specimens from OA patients (Supplementary Table S1). The Hospital for Special Surgery Knee-Rating Score (HSS) was employed for the grading of affected OA joints before arthroplasties.[42] Each specimen was divided into 2 parts, for immunohistochemistry or western blot analyses. The specimens were collected by a protocol that adhered to the tenets of the Declaration of Helsinki and was approved by the Ethics Committee of Chinese PLA General Hospital.

Mouse strains, tamoxifen induction, and NAC treatment
All mouse experimental protocols were designed according to the recommendation of the Beijing Experimental Animal Regulation Board (SYXK/JING/2005/0031). All mice were on the C57BL/6 genetic background and kept under specific pathogen-free conditions.

Genetically engineered mouse strains included transgenic *Col2a1-Cre* and *Col2a1-Cre^{ERT2}* mice,[8,25] conditional *PTEN^{fl/fl}*, *Akt1^{fl/fl}* and *ROSA^{EYFP}* mice.[8,43,44]

Experimental OA model was induced by destabilization of the medial meniscus (DMM) surgery performed on 8-week-old mice. Sham-operated mice were used as controls.[24] Male mice were used throughout this study.

For induction of Cre^{ERT2} activity, tamoxifen (Sigma, T5648, 0.1 mg·g⁻¹ body weight/day) was injected intraperitoneally into mice for 5 consecutive days.
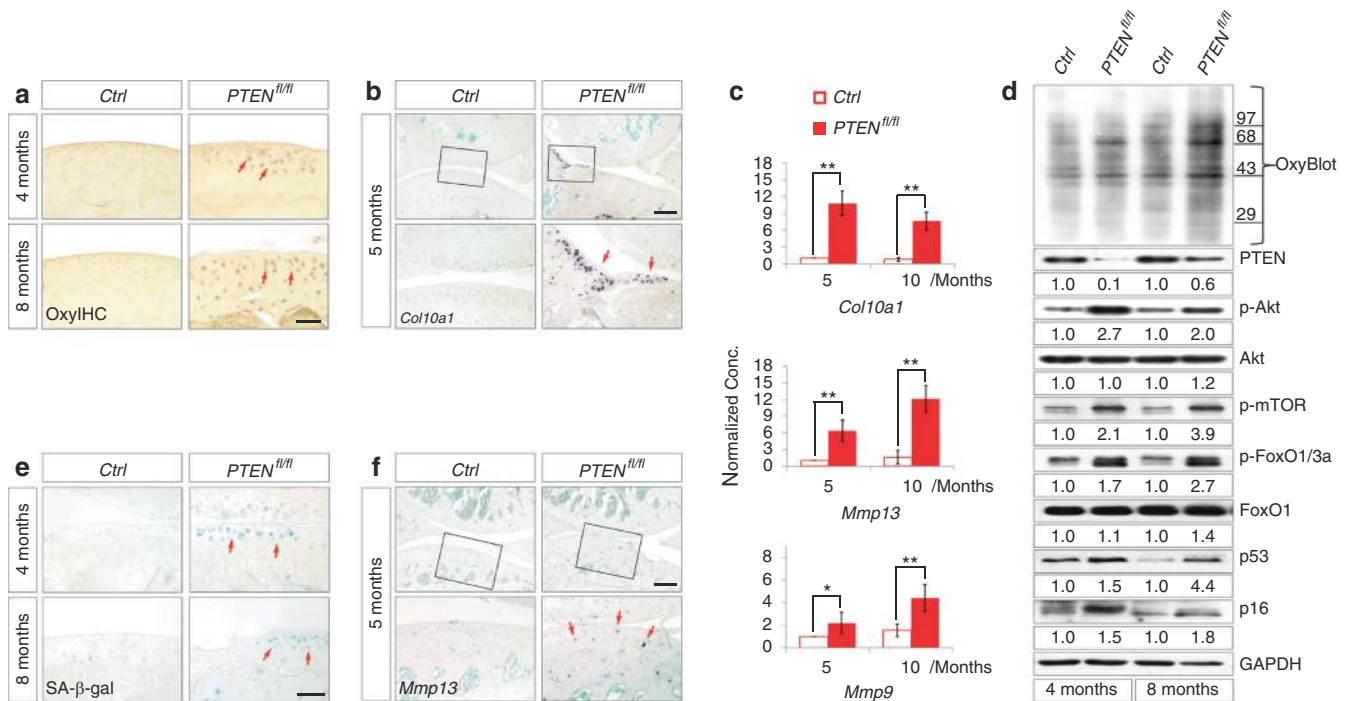
Fig. 5 Sustained Akt signaling in articular chondrocytes causes oxidative stress-related senescence. **a** Representative images of OxyIHC staining of articular cartilage from *Ctrl* and *PTEN^fl/fl* mice at 4 and 8 months (*n* = 4 per group). Red arrows denote the positive staining within articular chondrocytes of *PTEN^fl/fl* mice. **b** Representative images of *Col10a1* in situ hybridization analyses of knee joints from *Ctrl* and *PTEN^fl/fl* mice at 5 months (*n* = 3 per group). The framed area in each picture is shown below at a higher magnification. Red arrows denote the positively stained cells within the articular cartilage and meniscus of *PTEN^fl/fl* mice. **c** Representative real-time PCR analyses of *Col10a1*, *Mmp13*, and *Mmp9* expression in articular cartilage from *Ctrl* and *PTEN^fl/fl* mice at 5 and 10 months. Each value represents the mean ± SEM (*n* = 3 per group). *$P < 0.05$; **$P < 0.01$. **d** OxyBlot analysis for protein oxidation and western blot analyses for the levels of molecules involved in PTEN/Akt senescence axis. Samples were collected from articular cartilage of *Ctrl* and *PTEN^fl/fl* mice at 4 and 8 months. Quantitative densitometry results are shown below. The GAPDH protein serves as an endogenous normalizer. **e** Representative images of SA-β-gal staining of articular cartilage from *Ctrl* and *PTEN^fl/fl* mice at 4 and 8 months (*n* = 4 per group). Red arrows denote the senescent articular chondrocytes in *PTEN^fl/fl* mice. **f** Representative images of *Mmp13* in situ hybridization analysis of knee joints from *Ctrl* and *PTEN^fl/fl* mice at 5 months (*n* = 3 per group). The framed area in each picture is shown below at a higher magnification. Red arrows denote the positively stained cells within the articular cartilage of *PTEN^fl/fl* mice. Scale bars: 50 μm in (**a**) and (**e**), 250 μm in (**b**) and (**f**)

For NAC treatment, *Col2a1-Cre*; *PTEN^fl/fl* mice were randomly distributed into control and treatment groups. Mice in the treatment group were intragastrically administered freshly prepared 10 mg NAC (Sigma, A9165) in drinking water (adjusted to pH 7.0 using NaOH) every other day from 1 month to the time of sacrifice. Intragastric administration of 0.9% NaCl was applied to the control group in the same way.

μCT and 3D reconstruction

Mouse hind limbs were scanned by a high-resolution (5 μm cubic voxel size) μCT scanner (Skyscan 1172). 3D model visualization software (CTvox) was used to reconstruct the appearance of the tibial plateau. To allow visual characterization of the density distribution, 3D reconstruction images were color-coded based on Hounsfield Unit (HU) values, which refer to the respective grayscale values.

Histology, immunohistochemistry, in situ hybridization, OxyIHC, and SA-β-gal staining

For human articular cartilage, the specimens were fixed in 4% paraformaldehyde (PFA) at 4 °C for 2 days, decalcified in 0.5 mol·L⁻¹ EDTA in PBS for 2–3 weeks, dehydrated and embedded in paraffin. For mouse articular cartilage, whole knee joints with the tibia and femur were fixed in 4% PFA at 4 °C overnight, decalcified in 0.5 mol·L⁻¹ EDTA in PBS for 4–14 days, dehydrated and embedded in paraffin. The paraffin blocks were sectioned at 6 μm thickness.

For histopathologic scoring of mouse OA, a modified form of the OA Research Society International (OARSI) grading system was employed.[45] Briefly, serial sagittal sections of the medial joint at 30 μm intervals were obtained since the appearance of the inner margin of the medial meniscus, which yielded 10 slides per joint. Safranin O staining was then performed as described previously.[8] Articular cartilage degradation and subchondral bone changes were assessed in the medial tibial plateau by two blinded observers using an arbitrary grading scale of 0–6 for the severity of cartilage destruction and 0–3 for subchondral bone.[45] The total grades of 10 sections per joint were then summed to determine the OA score (maximum score of 90). Additional histopathologic grading methods were employed to evaluate synovial changes as well as subchondral bone thickening. The severity of synovial hyperplasia was scored on a grading scale of 0–3 for cell thickness (0 = 1 cells thick, 1 = 2–3 cells thick, 2 = 4–5 cells thick, and 3 = more than 6 cells thick).[46] The thickness of the subchondral bone plate, i.e., the distance between the osteochondral junction and the marrow space below the tibial plateau, was quantified in ImageJ software.[47,48] Osteophytosis was identified by safranin O staining of coronal sections of mouse knee joints and was graded by osteophyte size and osteophyte maturity. Briefly, osteophyte size was quantified by a grading scale of 0–3 (0 = no osteophytes, 1 = thickness similar to the adjacent cartilage, 2 = 1–3 times the thickness of the adjacent cartilage, and 3 = more than 3 times the thickness of the adjacent cartilage). Osteophyte maturity was assessed by a grading scale of 0–3 (0 = no osteophytes, 1 =
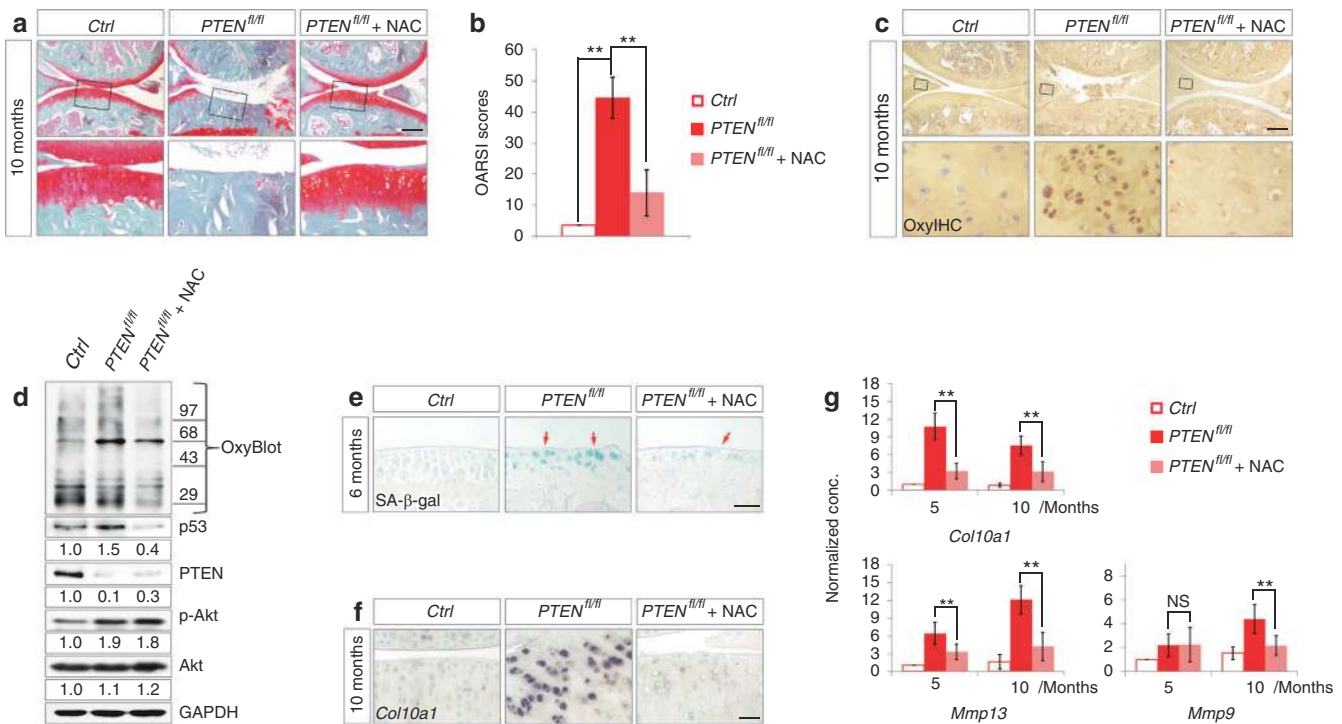
Fig. 6 NAC treatment relieves oxidative stress-induced chondrocyte senescence and mitigates OA phenotypes in *PTEN*-deficient mice. **a** Representative images of safranin O staining of articular sections of knee joints from 10-month-old *Ctrl* and *PTEN^fl/fl* mice as well as *PTEN^fl/fl* littermates treated with NAC for 9 months ($n = 12$ per group). **b** Quantified pathological changes of each group shown in (**a**). Each value represents the mean ± SEM ($n = 12$ per group). **$P < 0.01$. **c** Representative images of OxyIHC staining of knee joints from each group shown in (**a**) ($n = 3$ per group). The framed area in each picture is shown below at a higher magnification. **d** OxyBlot analysis for protein oxidation and western blot analyses for the levels of p53, PTEN, p-Akt, and Akt in articular cartilage from 6-month-old *Ctrl* and *PTEN^fl/fl* mice as well as *PTEN^fl/fl* littermates treated with NAC for 5 months. Quantitative densitometry results are shown below. The GAPDH protein serves as an endogenous normalizer. **e** Representative images of SA-β-gal staining of articular cartilage from 6-month-old *Ctrl* and *PTEN^fl/fl* mice as well as *PTEN^fl/fl* littermates treated with NAC for 5 months ($n = 3$ per group). Arrows denote senescent articular chondrocytes. **f** Representative images of *Col10a1* in situ hybridization analysis of knee joints from each group shown in (**a**) ($n = 3$ per group). **g** Representative real-time PCR analyses of *Col10a1*, *Mmp13*, and *Mmp9* expression in articular chondrocytes from 1-, 5- and 10-month-old knee joints. NAC was administered every other day from 1 month to the time of sacrifice. Each value represents the mean ± SEM ($n = 3$ per group). **$P < 0.01$. Scale bars: 250 μm in (**a**) and (**c**), 50 μm in (**e**) and (**f**)

predominant cartilage, 2 = mixed cartilage and bone with vascular invasion and endochondral ossification, and 3 = predominant bone).[49]

For immunohistochemistry, sections were rehydrated and subjected to antigen retrieval. The retrieval protocol for detecting GFP and phospho-Akt is as follows: slides were digested in 20 μg·mL^{-1} proteinase K at 37 °C for 10 min, followed by incubation in 10 mmol·L^{-1} citrate buffer (pH 6.0) at 50 °C for 16 h. The primary antibodies were monoclonal rabbit anti-GFP (Cell Signaling, 2 956, 1:200) and monoclonal rabbit anti-phospho-Akt (Ser473) (Cell Signaling, 4 060, 1:200). The signal was visualized with a Polink-1 HRP Kit for Rabbit (GBI Labs, D13–110) with DAB as the chromogen. Negative controls were performed using non-immunized IgG to replace the primary antibody (Fig. 1a and Supplementary Fig. S5a).

For OxyIHC, the knee joints were fixed in Methacarn fixative solution (10% glacial acetic acid, 30% trichloromethane, 60% methanol) at 4 °C overnight and decalcified in 0.5 mol·L^{-1} EDTA (without PFA) in PBS. Paraffin sections (6 μm) were used according to the Millipore OxyIHC^TM oxidative stress detection kit protocol (Millipore, S7450). Negative controls were performed with the Derivatization Control Solution from the Millipore OxyIHC^TM oxidative stress detection kit (Supplementary Fig. S5b).

For in situ hybridization, DIG-labeled antisense probes were generated from linearized template vectors with a DIG RNA Labeling Kit (Roche Life Science, 11277073910). In situ hybridization was performed using standard procedures.[50] The signal was

visualized with an AP-conjugated sheep-anti-DIG antibody (Roche Life Science, 11093274910, 1:2 000) with BCIP/NBT as the chromogen. Negative controls were performed using sense probes (Supplementary Fig. S5c and S5d).

For SA-β-gal staining, 10 μm cryosections of tibial articular cartilage were stained with the dye solution (1 mg·mL^{-1} X-Gal, 0.12 mmol·L^{-1} K$_3$Fe[CN]$_6$, 0.12 mmol·L^{-1} K$_3$Fe[CN]$_6$·3H$_2$O, 1 mmol·L^{-1} MgCl$_2$, pH 6.0) for 6 h–12 h according to the reported protocol.[51]

Western blot and OxyBlot analysis
Human articular cartilage specimens were ground in liquid nitrogen. The cartilaginous surface of dissected mouse knee joints was sliced by a fine knife under a stereomicroscope, collected and ground in liquid nitrogen. The sample for each genotype was obtained from 3–10 mice. Primary antibodies against PTEN (Cell Signaling, 9 188, 1:1 000), phospho-Akt (Ser473) (Cell Signaling, 4 060, 1:1 000), Akt (pan) (Cell Signaling, 4 685, 1:1 000), phospho-mTOR (Ser2448) (Cell Signaling, 5 536, 1:1 000), phospho-FoxO1 (Thr24)/FoxO3a (Thr32) (Cell Signaling, 9 464, 1:1 000), FoxO1 (Cell Signaling, 2 880, 1:1 000), p53 (Cell Signaling, 2 527, 1:500), p16 (Abcam, ab108349, 1:500) and GAPDH (Sigma-Aldrich, G8795, 1:5 000) were employed for Western blot analyses. OxyBlot was operated according to the Millipore OxyBlot^TM protein oxidation detection kit protocol (Millipore, S7150). Western blot results were quantified by densitometry using the ImageJ program. The value for each protein was normalized by its

corresponding GAPDH level. The normalized protein level in each control or sham group was then set as 1.0 (100%), and the littermates were presented as the ratio to the corresponding control or sham group.

Real-time PCR analyses

Ground articular cartilage obtained from 3–10 mice of each genotype was extracted using TRIZOL (Life Technologies, 15596-026). Total RNA was then reverse-transcribed using the mRNA Selective PCR Kit (Takara, RR025A). Real-time PCR was performed with the Roche LightCycler 2.0 system using a SYBR Select Master Mix (Life Technologies, 4472908) with four repeats for each sample. Expression values were normalized to *Hprt*.

Statistical analysis

The results are presented as the mean ± SEM. Quantitative data were tested for normality and homogeneity of variance. For comparisons between two groups, an unpaired Student's *t*-test was used. For multiple comparisons among more than two groups, data were analyzed by one-way analysis of variance (ANOVA), followed by Dunnett's test. Semiquantitative OA indices were analyzed using one-way ANOVA and the Kruskal–Wallis test, followed by Dunn's multiple comparison post hoc test. Differences were considered significant when the *P*-value was less than 0.05.

AUTHOR CONTRIBUTIONS

G.Y. and X.Y. contributed to the conception of the work; G.Y., J.X., L.Z., M.W., J.L. and Q.H. contributed to the acquisition of data; G.Y., Y.T., J.X., L.Z., J.L. and X.Y. contributed to the interpretation of data; and all authors contributed to drafting the manuscript and critical revision of its content. All authors gave their final approval for the submitted version of the manuscript and agreed to be accountable for all aspects of this work.

ADDITIONAL INFORMATION

The online version of this article (https://doi.org/10.1038/s41413-019-0062-y) contains supplementary material, which is available to authorized users.

Competing interests: The authors declare no competing interests.

REFERENCES

1. Glyn-Jones, S. et al. Osteoarthritis. *Lancet* **386**, 376–387 (2015).
2. Manning, B. D. & Toker, A. AKT/PKB Signaling: navigating the network. *Cell* **169**, 381–405 (2017).
3. Hollander, M. C., Blumenthal, G. M. & Dennis, P. A. PTEN loss in the continuum of common cancers, rare syndromes and mouse models. *Nat. Rev. Cancer* **11**, 289–301 (2011).
4. Chen, W. S. et al. Growth retardation and increased apoptosis in mice with homozygous disruption of the Akt1 gene. *Genes Dev.* **15**, 2203–2208 (2001).
5. Fukai, A. et al. Akt1 in murine chondrocytes controls cartilage calcification during endochondral ossification under physiologic and pathologic conditions. *Arthritis Rheum.* **62**, 826–836 (2010).
6. Peng, X. D. et al. Dwarfism, impaired skin development, skeletal muscle atrophy, delayed bone development, and impeded adipogenesis in mice lacking Akt1 and Akt2. *Genes Dev.* **17**, 1352–1365 (2003).
7. Ford-Hutchinson, A. F. et al. Inactivation of Pten in osteo-chondroprogenitor cells leads to epiphyseal growth plate abnormalities and skeletal overgrowth. *J. Bone Min. Res.* **22**, 1245–1259 (2007).
8. Yang, G. et al. PTEN deficiency causes dyschondroplasia in mice by enhanced hypoxia-inducible factor 1alpha signaling and endoplasmic reticulum stress. *Development* **135**, 3587–3597 (2008).
9. Rokutanda, S. et al. Akt regulates skeletal development through GSK3, mTOR, and FoxOs. *Dev. Biol.* **328**, 78–93 (2009).
10. Price, J. et al. Akt-1 mediates survival of chondrocytes from endoplasmic reticulum-induced stress. *J. Cell Physiol.* **222**, 502–508 (2010).
11. Starkman, B. G., Cravero, J. D., Delcarlo, M. & Loeser, R. F. IGF-I stimulation of proteoglycan synthesis by chondrocytes requires activation of the PI 3-kinase pathway but not ERK MAPK. *Biochem J.* **389**, 723–729 (2005).
12. Takeuchi, R. et al. Low-intensity pulsed ultrasound activates the phosphatidylinositol 3 kinase/Akt pathway and stimulates the growth of chondrocytes in three-dimensional cultures: a basic science study. *Arthritis Res Ther.* **10**, R77 (2008).
13. Greene, M. A. & Loeser, R. F. Function of the chondrocyte PI-3 kinase-Akt signaling pathway is stimulus dependent. *Osteoarthr. Cartil.* **23**, 949–956 (2015).
14. Xue, J. F., Shi, Z. M., Zou, J. & Li, X. L. Inhibition of PI3K/AKT/mTOR signaling pathway promotes autophagy of articular chondrocytes and attenuates inflammatory response in rats with osteoarthritis. *Biomed. Pharmacother.* **89**, 1252–1261 (2017).
15. Loeser, R. F. Aging processes and the development of osteoarthritis. *Curr. Opin. Rheumatol.* **25**, 108–113 (2013).
16. Jeon, O. H. et al. Local clearance of senescent cells attenuates the development of post-traumatic osteoarthritis and creates a pro-regenerative environment. *Nat. Med.* **23**, 775–781 (2017).
17. Ziegler, D. V., Wiley, C. D. & Velarde, M. C. Mitochondrial effectors of cellular senescence: beyond the free radical theory of aging. *Aging Cell.* **14**, 1–7 (2015).
18. Henrotin, Y., Kurz, B. & Aigner, T. Oxygen and reactive oxygen species in cartilage degradation: friends or foes? *Osteoarthr. Cartil.* **13**, 643–654 (2005).
19. Nakanishi, A., Wada, Y., Kitagishi, Y. & Matsuda, S. Link between PI3K/AKT/PTEN Pathway and NOX Proteinin Diseases. *Aging Dis.* **5**, 203–211 (2014).
20. Salminen, A. & Kaarniranta, K. Insulin/IGF-1 paradox of aging: regulation via AKT/IKK/NF-kappaB signaling. *Cell Signal.* **22**, 573–577 (2010).
21. Akasaki, Y. et al. FoxO transcription factors support oxidative stress resistance in human chondrocytes. *Arthritis Rheumatol.* **66**, 3349–3358 (2014).
22. Lehtinen, M. K. et al. A conserved MST-FOXO signaling pathway mediates oxidative-stress responses and extends life span. *Cell* **125**, 987–1001 (2006).
23. Zhao, X. et al. Peroxisome proliferator-activated receptor gamma coactivator 1alpha and FoxO3A mediate chondroprotection by AMP-activated protein kinase. *Arthritis Rheumatol.* **66**, 3073–3082 (2014).
24. Glasson, S. S., Blanchet, T. J. & Morris, E. A. The surgical destabilization of the medial meniscus (DMM) model of osteoarthritis in the 129/SvEv mouse. *Osteoarthr. Cartil.* **15**, 1061–1069 (2007).
25. Hilton, M. J., Tu, X. & Long, F. Tamoxifen-inducible gene deletion reveals a distinct cell type associated with trabecular bone, and direct regulation of PTHrP expression and chondrocyte morphology by Ihh in growth region cartilage. *Dev. Biol.* **308**, 93–105 (2007).
26. Luo, W. et al. Akt1 signaling coordinates BMP signaling and beta-catenin activity to regulate second heart field progenitor development. *Development* **142**, 732–742 (2015).
27. Davalli, P. et al. ROS, Cell Senescence, and Novel Molecular Mechanisms in Aging and Age-Related Diseases. *Oxid. Med Cell Longev.* **2016**, 3565127 (2016).
28. Kishimoto, H. et al. Induction of hypertrophic chondrocyte-like phenotypes by oxidized LDL in cultured bovine articular chondrocytes through increase inoxidative stress. *Osteoarthr. Cartil.* **18**, 1284–1290 (2010).
29. Morita, K. et al. Reactive oxygen species induce chondrocyte hypertrophy in endochondral ossification. *J Exp. Med.* **204**, 1613–1623 (2007).
30. Nakagawa, S. et al. N-acetylcysteine prevents nitric oxide-induced chondrocyte apoptosis and cartilage degeneration in an experimental model of osteoarthritis. *J. Orthop. Res.* **28**, 156–163 (2010).
31. Lin, Y. C. et al. Chondroprotective effects of glucosamine involving the p38 MAPK and Akt signaling pathways. *Rheuma. Int.* **28**, 1009–1016 (2008).
32. Chen, J. & Long, F. mTORC1 signaling controls mammalian skeletal growth through stimulation of protein synthesis. *Development* **141**, 2848–2854 (2014).
33. Zhang, Y. et al. Cartilage-specific deletion of mTOR upregulates autophagy and protects mice from osteoarthritis. *Ann. Rheum. Dis.* **74**, 1432–1440 (2015).
34. Baker, D. J. et al. Naturally occurringp16(Ink4a)-positive cells shorten healthy lifespan. *Nature* **530**, 184–189 (2016).
35. Baker, D. J. et al. Clearance of p16Ink4a-positive senescent cells delays ageing-associated disorders. *Nature* **479**, 232–236 (2011).
36. Nogueira, V. et al. Akt determines replicative senescence and oxidative or oncogenic premature senescence and sensitizes cells to oxidative apoptosis. *Cancer Cell.* **14**, 458–470 (2008).

37. Lin, K., Hsin, H., Libina, N. & Kenyon, C. Regulation of the Caenorhabditis elegans longevity protein DAF-16 by insulin/IGF-1 and germline signaling. *Nat. Genet.* **28**, 139–145 (2001).

38. Loeser, R. F. et al. Aging and oxidative stress reduce the response of human articular chondrocytes to insulin-like growth factor 1 and osteogenic protein 1. *Arthritis Rheumatol.* **66**, 2201–2209 (2014).

39. Yin, W., Park, J. I. & Loeser, R. F. Oxidative stress inhibits insulin-like growth factor-I induction of chondrocyte proteoglycan synthesis through differential regulation of phosphatidylinositol 3-Kinase-Akt and MEK-ERK MAPK signaling pathways. *J. Biol. Chem.* **284**, 31972–31981 (2009).

40. Collins, J. A. et al. Oxidative stress promotes peroxiredoxin hyperoxidation and attenuates pro-survival signaling in aging chondrocytes. *J. Biol. Chem.* **291**, 6641–6654 (2016).

41. Coleman, M. C. et al. Targeting mitochondrial responses to intra-articular fracture to prevent posttraumatic osteoarthritis. *Sci. Transl. Med.* **10**, eaan5372 (2018).

42. Hernandez-Vaquero, D. & Fernandez-Carreira, J. M.Relationship between radiological grading and clinical status in knee osteoarthritis. A multicentric study. *BMC Musculoskelet. Disord.* **13**, 194 (2012).

43. Guo, S. L. et al. Akt-p53-miR-365-cyclin D1/cdc25A axis contributes to gastric tumorigenesis induced by PTEN deficiency. *Nat. Commun.* **4**, 2544 (2013).

44. Srinivas, S. et al. Cre reporter strains produced by targeted insertion of EYFP and ECFP into the ROSA26 locus. *BMC Dev. Biol* **1**, 4 (2001).

45. Glasson, S. S., Chambers, M. G., Van Den Berg, W. B. & Little, C. B. The OARSI histopathology initiative–recommendations for histological assessments of osteoarthritis in the mouse. *Osteoarthr. Cartil.* **18**, S17–S23 (2010).

46. Jackson, M. T. et al. Depletion of protease-activated receptor 2 but not protease-activated receptor 1 may confer protection against osteoarthritis in mice through extracartilaginous mechanisms. *Arthritis Rheumatol.* **66**, 3337–3348 (2014).

47. Zhang, Z. et al. Curcumin slows osteoarthritis progression and relieves osteoarthritis-associated pain symptoms in a post-traumatic osteoarthritis mouse model. *Arthritis Res Ther.* **18**, 128 (2016).

48. Milz, S. & Putz, R. Quantitative morphology of the subchondral plate of the tibial plateau. *J. Anat.* **185**(Pt 1), 103 (1994).

49. Little, C. B. et al. Matrix metalloproteinase 13-deficient mice are resistant to osteoarthritic cartilage erosion but not chondrocyte hypertrophy or osteophyte development. *Arthritis Rheum.* **60**, 3723–3733 (2014).

50. Li, X. B. et al. Gastric Lgr5(+) stem cells are the cellular origin of invasive intestinal-type gastric cancer in mice. *Cell Res.* **26**, 838–849 (2016).

51. Debacq-Chainiaux, F., Erusalimsky, J. D., Campisi, J. & Toussaint, O. Protocols to detect senescence-associated beta-galactosidase (SA-betagal) activity, a biomarker of senescent cells in culture and in vivo. *Nat. Protoc.* **4**, 1798–1806 (2009).